MODELLING THE DYNAMICS OF A LOAD-HAUL-DUMP VEHICLE

B.J. Dragt, [*] **F.R. Camisani-Calzolari**[*, **] **and I.K. Craig**[*, ***]

[*] *Department of Electrical and Electronic Engineering, University of Pretoria, Pretoria, 0002, South Africa. Tel. +27 12 420 2472 Fax. +27 12 362 5000*
email:Bruce_Dragt@tuks.co.za
[**] *Tel. +27 12 420 2166 Fax. +27 12 362 5000*
email:Fernando.Camisani@eng.up.ac.za
[***] *Tel. +27 12 420 2172 Fax. +27 12 362 5000*
email:ICraig@postino.up.ac.za

Abstract: This paper provides an overview of the derivation of a dynamic model of a Load-Haul-Dump (LHD) vehicle. The model is derived using Lagrangian Dynamics and makes use of a simplified tyre model in an attempt to include the effect of basic tyre dynamics. Simulation results obtained from the vehicle model are provided and the results discussed and analysed.

Keywords: kinematics, dynamics, LHD vehicle, slip angles, articulated vehicle

1. INTRODUCTION

Load-Haul-dump(LHD) vehicles as shown in figure 1 are the work horses of the modern underground trackless mining environment. LHD vehicles are produced by a number of manufacturers and are available in various different models using either diesel or electric power and in various sizes. Typically the vehicles vary in length from 8 to 15 metres, weigh between 20000 - 75000kg with a transportation capacity of up to 25000kg.

The LHD vehicle is typically used for the transportation of fragmented ore from the stopes to an ore pass where the ore is transported by gravity to another handling point. The LHD and its operator move back and forth along the mine tunnel, which is typically a few hundred metres long, hauling the ore. The more repetitions of this cycle that are completed within a shift the higher the production. Therefore for reasons of safety as well as productivity it is desirable to automate LHD vehicles. In order to design a navigation system for an autonomous vehicle it is necessary to have a vehicle model that describes the vehicles position and other vehicle parameters through time.

The LHD vehicle poses unique modelling problems in that it's body consists of two parts connected together by means of an articulation joint. The front and rear wheel sets are fixed to remain parallel with the vehicle's body and vehicle steering is achieved by means of hydraulic actuators altering the articulation angle of the vehicle.

An articulated vehicle is preferable in the narrow environment of an underground mine tunnel because of its higher maneuverability as described by Altafini (1999).

Altafini (1999) has proven that the articulated vehicle can be modelled by a nonlinear system, with two inputs, namely speed and articulation angle, which is controllable. There are however some debates as to the complexity of the model required

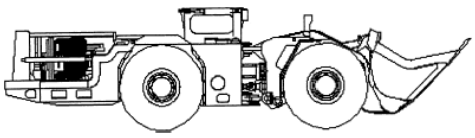

Fig. 1. An example of a typical LHD.

to successfully implement an autonomous vehicle navigation system, (Ridley and Corke, 2001), as increased model complexity places more stringent requirements on the computing power required on the actual vehicle in order to implement the navigation systems.

2. VEHICLE MODELLING

The main difference between the various vehicle models is whether the model is based purely on vehicle kinematic geometry or includes vehicle dynamics.

Due to the confined nature of the underground mining environment the LHD vehicles usually operate at relatively low speeds, typically below 28 km/h. For this reason the path-tracking problem has often been based on the kinematic model only, (Polotski and Hemami, 1997),(Dragt *et al.*, 2003). This assumption greatly reduces the complexity of the vehicle model as it is not possible to measure the amount of slip which has occurred during the vehicles motion. One approach which has been used to include the effect of slip is to estimate the amount of slip using an Extended Kalman Filter (EKF),(Scheding *et al.*, 1999). Details on Extended Kalman Filters can be found in (Brown, 1983).

2.1 Kinematic Modelling

In kinematic or low speed models the motion of a wheeled vehicle is determined only by the pure rolling of the wheels,(Genta, 1997). The velocities of the centres of all the wheels are assumed to be in the midplane of the wheel, that is there is no difference between the rotational plane of the tyre and the heading of the tyre. This means that the slip angles α are infinitesimally small. In this condition the wheels can exert no cornering force to balance the centrifugal force caused by cornering and therefore these model are only valid at infinitesimally small velocities,(Genta, 1997). Figure 2 illustrates the concept of a slip angle which is a dynamic effect which is present in all pneumatic tyres.

Figure 3 shows the kinematic vehicle geometry used by Scheding *et al.* (1999) to derive their vehicle model based on vehicle's kinematic geometry.

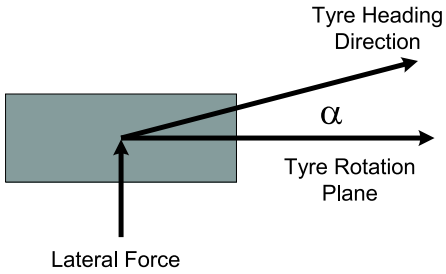

Fig. 2. Definition of slip angle α.

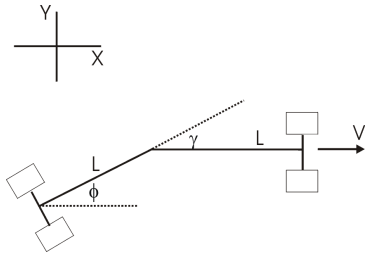

Fig. 3. LHD kinematic geometry.

Equations (1) is the model derived by Scheding *et al.* (1999) from kinematics only.

$$\begin{aligned} \dot{x} &= V cos\phi \\ \dot{y} &= V sin\phi \\ \dot{\phi} &= \frac{V tan(\frac{\gamma}{2})}{L} \end{aligned} \tag{1}$$

where x and y denote the position of the vehicle relative to some fixed global co-ordinate frame of reference, and L refers to the distance between the front and rear wheels of the vehicle and the articulation joint which is referred to as the half-length of the vehicle. The angle ϕ is the orientation of the vehicle with respect to the x-axis also referred to as the heading and γ is defined as the articulation angle of the vehicle. These equations are based on the assumption that the front and rear wheel velocities of the LHD are identical and that the articulation angle remains constant.

2.2 Dynamic Modelling

In order to model the vehicles dynamics it is necessary to take into account the generalised forces acting on the vehicle. Most of the forces acting on the vehicle are dependant on the tyre/road interaction in a complex nonlinear manner. The tyre forces at the tyre road interface can be resolved into lateral(cornering) and longitudinal(traction) forces at an assumed contact point. These forces then determine the slip angles of each tyre and wheel. It is however not possible to measure these slip angles and they therefore have to be estimated in some manner.

Scheding *et al.* (1999) makes use of an Extended Kalman Filter (EKF) to estimate these slip angles

in the vehicle model which includes the effect of slip. This is done by including only two slip variables (α and β), one for each axle into the kinematic vehicle model, as illustrated in figure 4. This approach is similar to what is commonly referred to as the single-track or bicycle model of a wheeled vehicle,(Gillespie, 1992). Simulation results for this modelling approach can be found in Dragt *et al.* (2004).

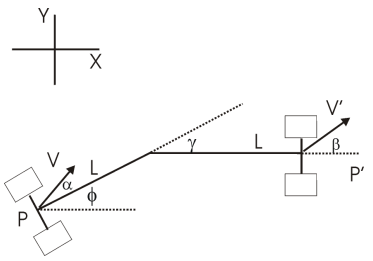

Fig. 4. LHD kinematic geometry indicated slip angles.

This approach does however have the shortcoming that the model is dependant on the accuracy of the statistical parameters used to estimate the slip variables in the error model of the Kalman filter. No detail is given by Scheding *et al.* (1999) on how these parameters where determined.

An alternative approach, and the one used here, to estimate the slip angles of the tyres is to make use of a characteristic of pneumatic tyres known as the cornering stiffness (C_α). Cornering stiffness is defined as the slope of the lateral force verses slip angle curve evaluated at zero slip angle,(Gillespie, 1992). It is possible to determine the cornering stiffness of a tyre and once this parameter is known, the slip angle of the tyre can be estimated based of the lateral force and vertical load being applied to the tyre. This approach can be applied to a bicycle or single-track model as used by Scheding *et al.* (1999) by using double the cornering stiffness so as to account for both wheels attached to a particular axle. Unfortunately these tyre characteristic measurements are not usually carried out on large tyres as used on an LHD vehicle. Therefore for the purposes of this model tyre data for a similar size tyre has been used until the measurements can be carried out. Alternatively a complex empirical tyre model can be used to determine the same parameters should more extensive information on the tyres be available. One example of an empirical tyre model is that of Baraket and Fancher (1989).

2.3 Dynamic Model Derivation

This section provides a summary of the derivation of the LHD vehicle dynamic model using Lagrangian dynamics. The same approach as described in (Wells, 1967) and (Chen and Tomizuka, 1997) is followed in this derivation.

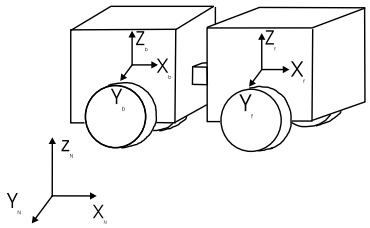

Fig. 5. Coordinate system used in model derivation.

The coordinate system is defined to characterise the motion on an articulated LHD vehicle. As shown in figure 5, X_n, Y_n, Z_n is the fixed global coordinate system. In applying the Lagrange method expressions for the kinetic and potential energies are obtained relative to this coordinate system. X_f, Y_f, Z_f are the coordinate system attached to the front unit of the LHD with Z_f position in such a way that it passes through the front units centre of gravity. Similarly X_r, Y_r, Z_r denote the position of the rear unit of the LHD vehicle. The motion of the front unit of the LHD can be described by the relative motion of the X_f, Y_f, Z_f coordinate system with respect to the X_n, Y_n, Z_n coordinate system. The motion of the rear unit of the vehicle can be characterised by describing the articulation angle between the front and rear units, or by describing the motion of the X_r, Y_r, Z_r coordinate system relative to the X_f, Y_f, Z_f coordinate system. Using this coordinate system a set of variables for the LHD vehicle can be introduced to as follows:

x_n : position of front unit's C.G. in x-direction on inertial coordinates
$\dot{x}_n$: velocity of front unit's C.G. in x-direction on inertial coordinates
y_n : position of front unit's C.G. in x-direction on inertial coordinates
$\dot{y}_n$: velocity of front unit's C.G. in x-direction on inertial coordinates
ϵ_1 : front unit's yaw angle with respect to inertial coordinate system
$\dot{\epsilon}_1$: front unit's yaw rate with respect to inertial coordinate system
ϵ_f : articulation angle between front and rear unit of vehicle
$\dot{\epsilon}_f$: rate of change of articulation angle between front and rear unit of vehicle

The vehicle rotational and translational velocities are then determined to be as follows for the front and rear units of the LHD vehicle.

$$V_{CG1/n} = \dot{x_n}\mathbf{i_n} + \dot{y_n}\mathbf{j_n} + 0$$
$$= (\dot{x_n}cos\epsilon_1 + \dot{y_n}sin\epsilon_1)\mathbf{i_f} + (-\dot{x_n}sin\epsilon_1 + \dot{y_n}cos\epsilon_1)\mathbf{j_f} \quad (2)$$

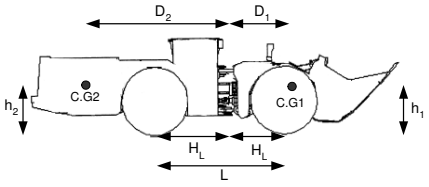

Fig. 6. Schematic diagram of vehicle parameters used in model.

$$V_{CG2/n}=V_{CG1/n}-D_1\frac{d}{dt}\mathbf{i_f}-d_1\frac{d}{dt}\mathbf{k_f}-D_2\frac{d}{dt}\mathbf{i_r}-d_2\frac{d}{dt}\mathbf{k_r}$$
$$V_{CG2/n}=V_{CG1/n}-D_1\epsilon_1\mathbf{j_f}-D_2(\dot{\epsilon_1}+\dot{\epsilon_f})\mathbf{j_r} \quad (3)$$

These equations are used in deriving the expressions for the kinetic and potential energies necessary to apply Lagrange's equations. It can be shown that the expression for the kinetic energy of the front and rear units of the vehicle are as shown is 5 and 6.

The change in potential energy (V) of the vehicle would be caused mainly by roll motion in the vehicle suspension as detailed in (Chen and Tomizuka, 1997). However due to the limited amount of suspension travel and the heavy loads carried by an LHD vehicle it was decided to neglect the effects of roll motion. Thus there is no change in potential energy.

$$V = 0 \quad (4)$$

The kinetic energy of the front unit (T_1) of the vehicle can be calculated from it's translational and rotational velocity as show in 5.

$$T_1 = \frac{1}{2}m_1{V_{CG1}}^2 + \frac{1}{2}\omega_f I_1 \omega_f \quad (5)$$

similarly the kinetic energy of the rear unit (T_2) can be calculated as

$$T_2 = \frac{1}{2}m_2{V_{CG2}}^2 + \frac{1}{2}\omega_r I_2 \omega_r \quad (6)$$

where the V_{CG1} and V_{CG2} are the translational velocities and ω_f and ω_r are the angular velocities of the front and rear unit of the LHD vehicle respectively.

The Lagrangian is therefore defined as

$$L = T_1 + T_2 - 0 \quad (7)$$

By using Lagrange's equations the following four dynamic equations can be obtained. Table 1 provides a description of the parameters used in the vehicle model and as indicated in figure 6.

$$\frac{d}{dt}\frac{\partial L}{\partial \dot{x_n}} - \frac{\partial L}{\partial x_n} = F_{gx_n} \quad (8)$$

Table 1. Parameters of vehicle model.

Parameter	Description
m_1	Mass of front unit
I_{x1}, I_{y1}, I_{z1}	Front unit moment of inertia
m_2	Mass of rear unit
I_{x2}, I_{y2}, I_{z2}	Rear unit moment of inertia
T_{w1}	Track width of front axle
T_{w2}	Track width of rear axle
$C_{\alpha f}$	Front tyre cornering stiffness
$C_{\alpha r}$	Rear tyre cornering stiffness
H_L	Distance from axle to articulation joint
L	Vehicle wheelbase
h_1, h_2	Heights of centre of gravity (CG)
D_1, D_2	Distance from joint to CG
d_1, d_2	Vertical distance from joint to CG

$$\frac{d}{dt}\frac{\partial L}{\partial \dot{y_n}} - \frac{\partial L}{\partial y_n} = F_{gy_n} \quad (9)$$

$$\frac{d}{dt}\frac{\partial L}{\partial \dot{\epsilon_1}} - \frac{\partial L}{\partial \epsilon_1} = F_{g\epsilon_1} \quad (10)$$

$$\frac{d}{dt}\frac{\partial L}{\partial \dot{\epsilon_f}} - \frac{\partial L}{\partial \epsilon_f} = F_{g\epsilon_f} \quad (11)$$

where $F_{gx_n}, F_{gy_n}, F_{g\epsilon_1}$ and $F_{g\epsilon_f}$ refer to the generalised external forces acting on the vehicle. These external forces acting on the vehicle consist of the tyre/road interface. In order to calculate the generalised forces, expressions for the generalised forces are derived in terms of longitudinal and lateral components of the tyre forces as indicated in figure 7. The full derivation of these forces is too long to be shown here.

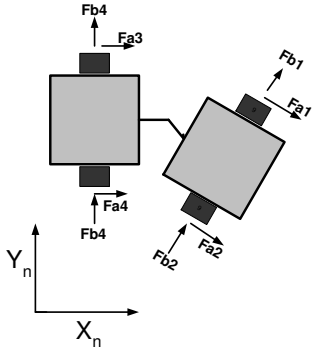

Fig. 7. Definition of tyre forces in Cartesian Coordinates.

Equations 8, 9, 10,11 can be combined with the expressions derived for the generalised forces and after some manipulation written in the following form.

$$\left(\ddot{\mathbf{q}}\right) = -\mathbf{M^{-1}h}(\mathbf{q}, \dot{\mathbf{q}}) + \mathbf{M^{-1}F_g} \quad (12)$$

where

$$\mathbf{q} = \begin{pmatrix} x \\ y \\ \epsilon_1 \\ \epsilon_f \end{pmatrix} \quad (13)$$

$\mathbf{M}$ is the inertia matrix and $\mathbf{F_g}$ are the generalised forces acting on the wheels.

Equation 12 can be combined with the parameters from the tyre model to determine the generalised forces and perform a simulation of the vehicles dynamics by integrating the state variables.The results are shown in the next section.

3. SIMULATION

This section provides simulation results for the derived LHD vehicle model. The simulations where performed in Matlab and the parameters indicated in table 1 are based on the vehicle parameters of a Sandvik-Tamrock EJC 245 LHD, which has a tramming capacity of 11000Kg,(*Sandvik Mining and Construction Global Site*, 2003). The simulations were however performed based on the vehicles empty weight and the vehicle is assumed to be operating on level terrain with a friction coefficient of 0.7. Parameters which where not available were estimated based on vehicle dimensions.

Due to a lack of availability of complete tyre data the simulations were performed using average values of the tyre cornering stiffness which are valid for tyre slip angles of up to 5 degrees. These parameters were used for the entire simulation. The full dynamic tyre model where parameters vary according to loading and velocities will be implemented when the complete tyre data are made available.

As the main emphasis of the dynamic model is on the cornering performance of the LHD vehicle the simulations where carried out at a constant velocity of 18 km/h. Figure 8 shows a plot of the commanded rate of change of steering input against time. At time $t = 2$ seconds the vehicle starts turning to the left once the articulation angle has reached full lock in the one direction the vehicle starts turning back in the other direction. Figure 9 shows the path followed by the vehicle for the rate of change of the steering angle $\dot{\epsilon_f}$ shown in figure 8.

Figure 10 shows the slip angles for each tyre determined by the vehicle model for the motion of the vehicle. As can be seen from figure 10 the slip angles exceed 5 degrees towards the end of this motion and thus the cornering forces predicted by the tyre model lose accuracy. This results in the vehicle model being biased towards an understeer characteristic as the lateral forces generated during cornering will increase with increased slip angles. This is due to the fact that C_α typically increases linearly with increased slip angle up to a certain maximum value at large slip angles and

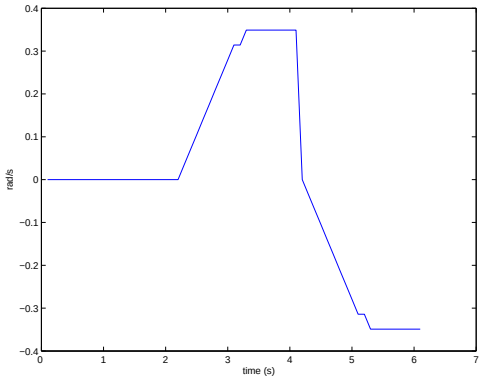

Fig. 8. Plot of rate of change of articulation angle ($\dot{\epsilon_f}$) in radians per second verses time.

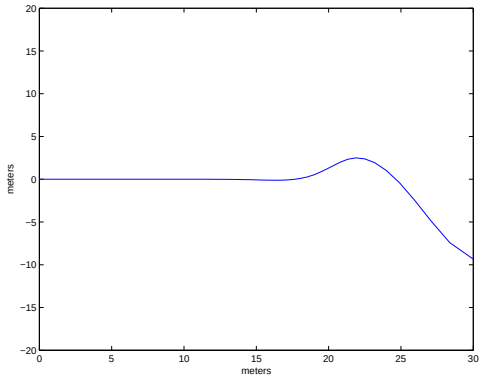

Fig. 9. Plot of vehicle trajectory.

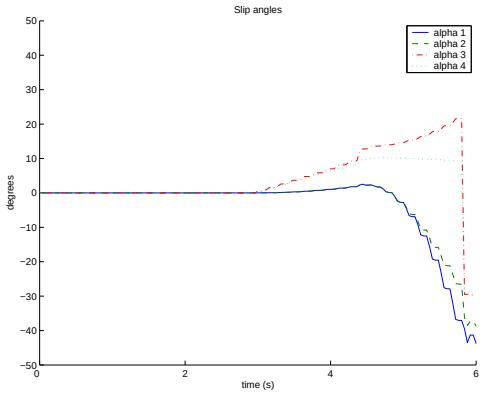

Fig. 10. Plot of slip angles α_1, α_2, α_3 and α_4 verses time.

the lateral force generated by the ith tyre (F_{yi}) is given by equation 13,(Genta, 1997).

$$F_{yi} = C_\alpha.\alpha_i \tag{13}$$

4. CONCLUSIONS AND FUTURE WORK

In conclusion to determine the cornering forces acting on the vehicle is probably one of the most difficult tasks. The lateral forces generated by the tyres are entirely dependant on the characteristics of the tyre - primarily the cornering stiffness C_α. The results shown in the previous section are thus

highly dependant on the parameter C_α used in the simulation and are only as accurate as the estimate of this value. The simulations do however show the performance of the vehicle under the particular operating condition assumed. Although this simulation was based on a simplified tyre model and certain vehicle parameters had to be estimated the results appear to be realistic.

In future work a more advanced and accurate tyre model will be added to the vehicle model as well as the actual values of the estimated vehicle parameters. The model will also be expanded to take into account the effect of pitch on the vehicle dynamics. This model will then be validated against tests performed on an LHD vehicle above ground using GPS measurements to record the vehicles movements. Any necessary tuning of the model can then be performed.

5. ACKNOWLEDGMENTS

This material is based upon work supported by the National Research Foundation under grant number 2053268. The authors also wish to thank Dr. Gunter Metzner of De Beers Consolidated Mines for his contribution to this research project.

REFERENCES

Altafini, C. (1999). Why to use an articulated vehicle in underground mining operations ?. In: *Proceedings of the 1999 IEEE International Conference on Robotics and Automation*. Detroit.

Baraket, Z. and P. Fancher (1989). Representation of truck tire properties in braking and handling studies: The influence of pavement and tire conditions on frictional characteritics. *Technical Report University of Michigan Transportation Research Institute*.

Brown, R.G (1983). *Introduction to Random Signal Analysis and Kalman Filtering*. John Wiley and Sons. New York.

Chen, C. and M. Tomizuka (1997). Modelling and control of articulated vehicles. *California PATH research report*.

Dragt, B.J., I.K. Craig and F.R. Camisani-Calzolari (2003). Autonomous underground mine vehicles. In: *The 1st African Control Conference (AFCON2003)*. Cape Town, South Africa. pp. 369–374.

Dragt, B.J., I.K. Craig and F.R. Camisani-Calzolari (2004). Modelling of an autonomous underground mine vehicle. In: *Preprints of The 11th IFAC Symposium on Automation in Mining, Mineral and Metal Processing(MMM2004)*. Nancy, France.

Genta, G. (1997). *Motor Vehicle Dynamcis, Modeling and Simulation, Series on advances in Mathematics for Applied Sciences - Vol. 43*. World Scientific. London.

Gillespie, T.D (1992). *Fundamentals of Vehicle Dynamics*. Society of Automotive Engineers, Inc.. Warrendale, PA.

Polotski, V. and A. Hemami (1997). Control of articulated vehicle for mining applications: Modeling and laboratory experiments. In: *Proceedings of the 1997 IEEE International Conference on Control Applications*. Hartford, CT.

Ridley, P. and P. Corke (2001). Autonomous control of an underground mine vehicle. In: *Proceedings 2001 Australian Conference on Robotics and Automation*. Sydney.

Sandvik Mining and Construction Global Site (2003). http://www.smc.sandvik.com/. Last visited: September 2003.

Scheding, S., G. Dissanayake, E.M. Nebot and H. Durrant-Whyte (1999). An experiment in autonomous navigation of an underground mine vehicle. *IEEE Transactions on robotics and Automation* **15 no.1**, 127 –146.

Wells, D.A (1967). *Schaums's Outline of theory and problems of Lagrangian Dynamics*. McGraw-Hill. New York.